Am J Transl Res 2022;14(1):150-165
www.ajtr.org /ISSN:1943-8141/AJTR0133418

*Original Article*

# Effects of extracellular histones on left ventricular diastolic function and potential mechanisms in mice with sepsis

Lijun Wang[1,2*], Ziyi Wang[2,3*], Xing Liu[1], Yue Zhang[1], Manman Wang[4], Xue Liang[1], Guangping Li[1]

*[1]Department of Cardiology, Tianjin Key Laboratory of Ionic-Molecular Function of Cardiovascular Disease, Tianjin Institute of Cardiology, The Second Hospital of Tianjin Medical University, Tianjin 300211, People's Republic of China; [2]Department of Emergency Medicine, Tianjin Medical University General Hospital, Tianjin 300052, People's Republic of China; [3]School of Clinical Medicine, Tsinghua University, Beijing 100084, People's Republic of China; [4]Department of Cardiology, Affiliated Hospital of Jining Medical University, Jining 272000, Shandong, People's Republic of China. [*]Equal contributors.*

Received March 23, 2021; Accepted October 14, 2021; Epub January 15, 2022; Published January 30, 2022

**Abstract:** Objective: Extracellular histone (EH) is involved in the development of septic myocardial injury (SMI). In this study, we explored whether EH could induce left ventricular diastolic dysfunction (LVDD) in sepsis, and investigated the potential mechanisms through *in vivo* and *in vitro* experiments using animal models. Methods: The ratio between E-wave and A-wave (E/A ratio), left ventricular end diastolic volume, and isovolumic relaxation time (IVRT) were measured in cecal ligation and perforation (CLP)- and EH-treated male C57BL/6J mice using echocardiography. The protein and mRNA levels of apoptosis-related proteins (cleaved caspase-3, Bcl-2, and Bax) and cardiac troponin T (cTnT) in the left ventricular tissue/cardiomyocytes were measured using enzyme-linked immunosorbent assay, qRT-PCR, and western blotting. Cardiomyocyte apoptosis was detected by flow cytometry. Results: CLP mice presented with LVDD, which was accompanied by increased circulating histones, cTnT and Bax protein levels. Circulating histones were correlated with cTnT, Bax, IVRT, and E/A ratio in CLP mice. Intraperitoneal injection of EH resulted in LVDD in mice. EH induced cardiomyocyte apoptosis, and histone neutralizing agents improved SMI and protected mice against CLP- and EH-induced death. Conclusion: EH is involved in septic LVDD, and this alteration might be associated with EH-induced apoptosis. EH may serve as a potential therapeutic target for SMI.

**Keywords:** Extracellular histones, septic myocardial injury, left ventricular diastolic dysfunction, apoptosis, Bax

## Introduction

Sepsis is a life-threatening organ dysfunction caused by a dysregulated host response to infection [1]. The heart is vulnerable to sepsis. Sepsis can result in cardiac insufficiency, dysfunction of ventricular dilatation, contraction, and relaxation, and cardiac function involvement, referred to as septic myocardial injury (SMI) [2, 3]. Patients with SMI are at a high risk of multiple organ failure and have high mortality [4]. In echocardiography, SMI presents as systolic or diastolic dysfunction of the right and left sides of the heart, or global or regional wall motion abnormalities [5, 6]. Left ventricular diastolic dysfunction (LVDD) is a common but easily overlooked complication in patients with severe sepsis or septic shock, and has a worse prognosis than systolic dysfunction [2, 7-10].

Recent research has demonstrated that the apoptosis process plays a critical role in SMI pathogenesis [11-13]. Both extrinsic and intrinsic apoptotic pathways exist in septic cardiomyocytes [14, 15]. Cardiomyocyte apoptosis can induce the cleavage of cardiac myofilament components, resulting in diastolic dysfunction. Thus, apoptosis-targeted therapy can improve SMI [11, 16, 17]. An increasing number of studies have found that extracellular histones (EH) are implicated in SMI [18-21]. Importantly, EH can cause apoptosis at an early stage and arrhythmias (including sinus bradycardia and ventricular bigeminy) [8, 19]. In the myocardi-

um, binucleated and polyploid cardiomyocytes have high concentrations of histones [22]. Once the myocardium is damaged, large amounts of histones are released, leading to massive apoptosis of cardiomyocytes [18]. Studies have reported that circulating histone levels are significantly elevated in patients with sepsis, especially those who do not survive; therefore, it could serve as a prognostic biomarker [8, 18, 23-27]. In mice, circulating histones can be detected 6 h after cecal ligation and perforation (CLP), and persist for 24 h, followed by a reduction [19]. EH concentration in the spleen, lung, liver, and kidney reached a peak at 8 h, whereas it peaked at 4 h in the heart, indicating that the heart suffered from EH-induced injury earlier than the other organs [28]. Anti-histone therapy can significantly improve the left ventricular remodeling and outcomes in mice with sepsis [19, 29]. However, whether EH can induce LVDD in sepsis and its potential mechanisms remain unclear.

In the present study, we investigated the effect of EH on LVDD in sepsis animal models via *in vivo* and *in vitro* experiments. In addition, the potential mechanisms were explored. Our research aimed to reveal a new mechanism of SMI pathogenesis.

## Materials and methods

### *Animal experiments*

Adult male C57BL/6J mice (6-8 weeks old) weighing 19-21 g were purchased from the Peking University Experimental Animals Center (Beijing, China). They were housed in a pathogen-free environment at the animal center of Tianjin Medical University and acclimated to their surroundings for 1 week. Standard mouse chow and water were available ad libitum during the experiment. The experimental protocols were approved by the Animal Welfare Ethics Committee of the Tianjin Medical University General Hospital (IRB2021-DW-20).

Sepsis was induced by CLP, as previously described [30]. Briefly, the mice were anesthetized with an intraperitoneal injection of 3% tribromoethanol. After midline incision, the cecum was exposed and ligated at 2/3 of the distal pole. The ligated cecum was punctured with an 18-gauge needle, and a small portion of feces was extruded. The abdomen was closed using 4-0 sutures. Sham animals underwent the same procedures, except for the ligation and puncture of the cecum. After surgery, all animals were subcutaneously injected with 1 mL of normal saline (37°C) for fluid resuscitation.

Unfractionated heparin (UFH; Biochem Pharmaceutical, Tianjin, China) and antithrombin affinity-depleted heparin (AADH) were used as EH-neutralizing reagents. Mice were randomly assigned to (1) sham, CLP, and CLP + UFH groups, and (2) control, EH, EH + UFH, and EH + AADH groups. In the sham, CLP, and CLP + UFH groups, UFH (3 mg/kg; Biochem Pharmaceutical) was intraperitoneally injected at 4 h and 16 h after CLP, and the left ventricular function was determined by echocardiography at 6 h and 24 h after CLP. Then, the mice were euthanized by dislocation of the cervical vertebrae to collect serum and left ventricular tissues subsequently (**Figure 1A**). Hematoxylin-Eosin (HE) staining of left ventricular tissues was performed for left ventricular tissues. In the control, EH, EH + UFH, and EH + AADH groups, the left ventricular function was assessed at 0.5, 1, 1.5, and 3 h after intraperitoneal injection of EH (50 mg/kg; 1022356-5001; Roche, Indianapolis, IN, USA) [8], respectively. UFH and AADH (3 mg/kg) were injected intraperitoneally 30 min before the EH injection [31].

### *Cell culture*

HL-1 cardiomyocytes were obtained from our laboratory and cultured in Claycomb medium (51800C; Sigma, San Francisco, USA) containing 10% fetal bovine serum (10091148; Gibco, Grand Island, NY, USA), 2 mM/L L-glutamine, 100 U/mL penicillin G, and 100 μg/mL streptomycin in a humidified incubator (37°C) with 5% $CO_2$. Cardiomyocytes were seeded in six-well tissue culture plates at $10\times10^6$ cells/well and grown to confluence. Protein, mRNA, or cell supernatant were extracted at the designated time after administration of EH (100 μg/mL), lipopolysaccharide (LPS, 1 μg/mL), or UFH (200 μg/mL) according to different experimental requirements [8, 31, 32].

### *Enzyme-linked immunosorbent assay (ELISA)*

For ELISA analysis, the cell supernatants of cardiomyocytes were collected and the expression levels of tumor necrosis factor α (TNF-α), inter-

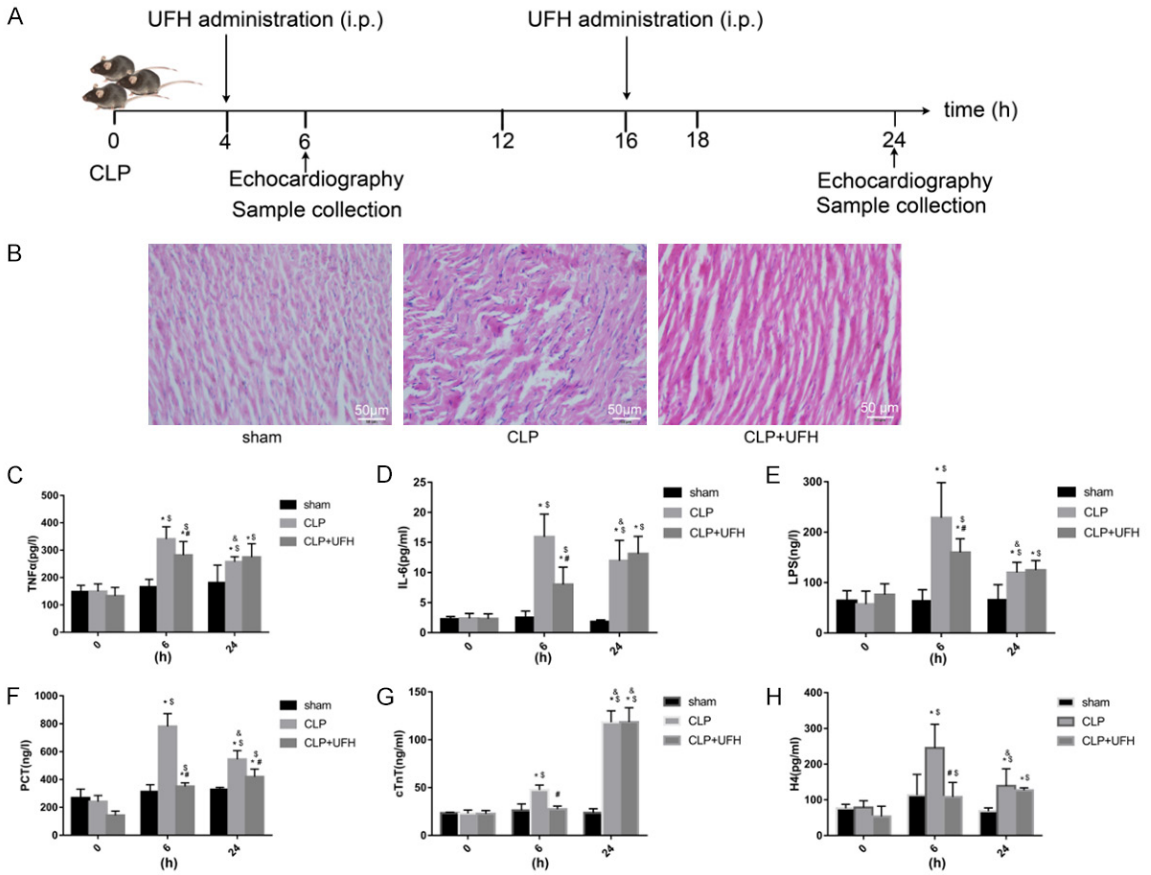


**Figure 1.** Comparison of different serum protein levels at designated time points. The flowchart of procedures in model group (A). Hematoxylin-Eosin (HE) staining of left ventricular tissues (200×) in sham, CLP and CLP + UFH groups (B). Serum protein levels of TNFα (C), IL-6 (D), LPS (E), PCT (F), cTnT (G) and H4 (H) in the sham, CLP, and CLP + UFH groups at 6 h or 24 h after CLP. UFH (3 mg/kg) was intraperitoneally injected at 4 h and 16 h after CLP. Values are presented as the mean ± SD (n=3). $^{*}$P<0.05 vs. sham group at the same time; $^{\#}$P<0.05 vs. CLP group at the same time. $^{\$}$P<0.05 vs. 0 h in the same group; $^{\&}$P<0.05 vs. 6 h in the same group. CLP, cecal ligation and puncture; UFH, unfractionated heparin; PCT, procalcitonin; LPS, lipopolysaccharide; H4, circulating histone h4.

leukin-6 (IL-6), procalcitonin (PCT), LPS, caspase-3, Bax, Bcl-2 and cardiac troponin T (cTnT) were quantified using commercially available ELISA kits (Guangrui Biological Technology, Shanghai, China). The same method was used for the serum/plasma analysis of the CLP mice.

*Flow cytometric analysis*

The apoptotic ratio was determined by flow cytometry with Annexin V-FITC/7AAD staining (640922; Biolegend, San Diego, CA, USA). After experimental treatment, cardiomyocytes were collected, washed with calcium-free phosphate-buffered saline, and resuspended in binding buffer. The cardiomyocytes were then treated with Annexin V-FITC and 7AAD for 15 min in the dark, and analyzed using a Beckton-Dickinson flow cytometer (Navios; Beckman Coulter, Brea, CA, USA).

*RNA extraction and quantitative real-time RT-PCR (qRT-PCR)*

Total RNA was isolated using TRIzol (Invitrogen, Carlsbad, CA, USA) to analyze the expression levels of caspase-3, Bax, and Bcl2 in cardiomyocytes and heart tissues. qRT-PCR was performed using a FastQuant RT kit (with gDNase) and TransStart® Top Green QpcrSuperMix (TransGen Biotech, Beijing, China). Amplification was conducted by denaturation at 95°C for 10 min, followed by 40 cycles of 95°C for 30 s, 60°C for 30 s, and 72°C for 30 s on an Applied Biosystems 7500 Fast Real-Time PCR system. Relative mRNA expression levels were normal-

ized to glyceraldehyde 3-phosphate dehydrogenase (GAPDH) using the $2^{-\Delta\Delta Ct}$ method. All PCR experiments were performed in triplicates and repeated at least three times. The primers used for qRT-PCR were GAPDH: forward TGCACCACCAACTGCTTAG, reverse GATGCAGGGATGATGTTC; Bax: forward AGCTGCAGAGGATGATTGCT, reverse ATGGTTCTGATCAGCTCGGG; Bcl-2: forward CCACCTGTGGTCCATCTGA, reverse GACTGGACATCTCTGCGAA; Caspase-3: forward TGCTCACGAAAGAACTGTACT, reverse GACAGCTTTCTCATTTGGCATA.

*Western blotting*

Total proteins were extracted from cultured cardiomyocytes or left ventricular tissues using a lysis buffer. The cardiomyocytes were boiled for 10 min, centrifuged at 13,000 rpm for 5 min, and then subjected to 10% sodium dodecyl sulfate-polyacrylamide gel electrophoresis. The proteins were transferred to nitrocellulose membranes (Amersham Biosciences, Piscataway, NJ, USA) and blocked for 1 h in Tris-buffered saline with Tween 20 containing 5% BSA at room temperature (25-30°C). Immunoblotting was performed by incubating the membranes with primary antibodies against caspase-3 (1:1000; 9662s; CST, USA), cleaved caspase-3 (1:1000; ab49822; Abcam, Cambridge, MA, USA), Bax (1:500; ab32503; Abcam), and Bcl-2 (1:1000; ab692; Abcam), followed by incubation with the appropriate secondary antibodies, including goat anti-mouse IgG-H&L (1:10000; ab136815; Abcam) and goat anti-rabbit IgG-H&L (1:10000; ab136817; Abcam). After washing, protein signals were visualized using an enhanced chemiluminescence detection system (Millipore, Billerica, MA, USA).

*Transthoracic echocardiography*

Echocardiography was performed according to the methodology described in a previous study [5]. The mice were anesthetized with 0.8% isoflurane using an anesthetic machine during recording. The standard techniques for obtaining M-mode, two-dimensional, and Doppler echocardiograms were performed by the same cardiologist who was blinded to the experimental details. Imaging was performed using a Vevo 2100 Imaging System (FUJIFILM VisualSonics, Inc., Toronto, Ontario, Canada) equipped with an MS400 (30-45 MHz) transducer. The ratio between E-wave and A-wave (E/A ratio), isovolumic relaxation time (IVRT), and left ventricular end diastolic volume (LVEDV) were used to assess the left ventricular diastolic function. Stroke volume, cardiac output (CO), and ejection fraction (EF) were used to determine the systolic function. IVRT was measured from the apical five-chamber view using Doppler flow imaging [5]. Mitral valve E and A wave inflow velocities were sampled at the tips of the mitral valve leaflets from the apical 4-chamber view. Left ventricular length, used for the calculation of the left ventricular end systolic and diastolic volumes, was measured from the parasternal long axis.

*Blood samples*

Blood samples were collected at a specified time, and a one-tenth volume of 3.2% sodium citrate or ethylene diamine tetraacetic acid was added to prevent coagulation. Prothrombin time (PT) and activated partial thromboplastin time (APTT) were immediately measured. The other plasma samples were centrifuged at 3000 rpm for 20 min at room temperature and stored at -80°C until subsequent analyses.

*Statistical analysis*

Continuous data values are expressed as the mean ± standard deviation, and categorical data are presented as frequencies and percentages. Data were analyzed by one-way analysis of variance followed by Dunnett's or Tukey's multiple comparison tests, or chi-square test, as appropriate. The survival rate was analyzed using the Kaplan-Meier method. Circulating histones-left ventricular diastolic function linear correlation was analyzed using Spearman's rank correlation. Statistical analyses were performed using IBM SPSS Statistics for Windows (version 23.0, IBM Corp, Armonk, NY, USA) and GraphPad Prism 7.0 for Windows (GraphPad Software Inc., La Jolla, CA, USA). Statistical significance was set at a two-tailed *P*-value of $<0.05$.

## Results

*Left ventricular diastolic function was changed in CLP- and EH-treated mice*

Six hours after the CLP operation, the mice presented with lethargy, diarrhea, polypnea, and piloerection. HE staining demonstrated that the

myocardial arrangement of mice in CLP group was disordered, with inflammatory exudation accompanied by cell swelling (**Figure 1B**). ELISA showed increased levels of TNFα, IL-6, LPS, and PCT in CLP group compared with those in sham operation group (P<0.05; **Figure 1C-F**), suggesting that the mouse model mimicked the general clinical characteristics of sepsis. As shown in **Figure 1G** and **1H**, the circulating cTnT level and histone h4 in CLP mice were significantly increased compared with those in sham group at 6 h and 24 h after CLP (P<0.05, **Figure 1G**, **1H**).

In addition, LVEDV in the CLP group decreased significantly compared to the sham operation mice (P=0.002), suggesting that CLP could decrease the left ventricular filling capacity. Additionally, IVRT increased (P<0.001) and the E/A ratio significantly decreased (P=0.001) in the CLP group compared to the sham group (Figures S1, **2A** and **3A**). The results showed that LVDD appeared 6 h after CLP induction in mice. Besides, we found that serum levels of the circulating histone h4 and cTnT were elevated parallelly and concomitantly after 6 h of CLP induction compared to the sham group (both P<0.001) (**Figure 1G**, **1H**). There were significant correlations between the circulating histone h4 and cTnT ($r_s$=0.641, P=0.025), IVRT ($r_s$=0.804, P<0.001), or E/A ratio ($r_s$=-0.608, P=0.003). cTnT is a sensitive and specific biomarker of SMI (Langhorn and Willesen 2016). Therefore, the increase of circulating histone h4 might result in myocardial injury and LVDD in CLP mice.

To verify the effects of EH on the left ventricular diastolic function in mice, cardiac function was observed at designated times after EH stimulation. The results showed that the left ventricular diastolic function was not affected by 25 mg/kg of EH; however, it changed significantly in the 50 mg/kg EH at 0.5 h treatment, until 3 h, and the most significant alteration occurred at 1.5 h. IVRT was increased (P=0.001), E/A ratio was decreased (P=0.03), and LVEDV was decreased (P=0.001) significantly compared to the controls (Figures S2, **2B** and **3B**). These alterations were similar to those observed in CLP mice, indicating that EH could induce LVDD. However, the heart rate was increased in CLP mice (**Table 1**), whereas it was slightly decreased in the EH-treated mice (P=0.074).

As for systolic function, increased EF and decreased CO were found in mice at 6 h after CLP (Figures S1 and **2A**; **Table 1**). However, both EF and CO were significantly decreased in EH-treated mice at multiple time points (both P<0.05), demonstrating that EH affected both systolic and diastolic functions in mice (Figures S2 and **2B**).

*Histone neutralizing agents attenuated myocardial dysfunction and improved survival rate in CLP- or EH-treated mice*

UFH was used as EH-neutralizing reagents in mice. As displayed in **Figure 1C-H**, TNFα, IL-6, LPS, PCT, circulating cTnT and histone h4 levels were significantly decreased in CLP + UFH group, compared with those in CLP group (P<0.05), indicating that the general clinical characteristics of sepsis were partly relieved by UFH. As expected, echocardiography showed that left ventricular diastolic function was significantly improved (IVRT decreased, whereas LVEDV and E/A ratio increased; all P<0.05), and the left ventricular systolic function was also ameliorated (Figures S1 and **2A**).

Compared to the EH group, the left ventricular diastolic function was improved in the UFH and AADH groups (Figures S2, **2C** and **3A**). Unlike CLP mice, LVEF, CO, and Tei index were significantly improved after UFH administration (all P<0.05) (Figures S2 and **2C**).

To further confirm whether UFH or AADH protected EH-treated mice from death, 40 mice were divided into four groups: control, EH, EH + UFH, and EH + AADH groups. Both UFH and AADH (3 mg/kg, once every 12 h, 3 days in total) groups were intraperitoneally injected as previously described [32, 33]. Survival was observed at 12, 24, 36, 48, 72, and 96 h after EH administration. As shown in **Figure 3C**, UFH and AADH prevented the death of EH-treated mice. Moreover, five mice presented hemorrhage in the EH + UFH group, whereas only one hemorrhage occurred in the EH + AADH group ($x^2$=3.200, P=0.074).

To verify the non-anticoagulant effects of AADH, blood was added into sodium citrate (1:9 ratio, 3.2% sodium citrate) for PT and APTT measurement at 1.5 h after histone injection. AADH did not prolong APTT, demonstrating that its anti-

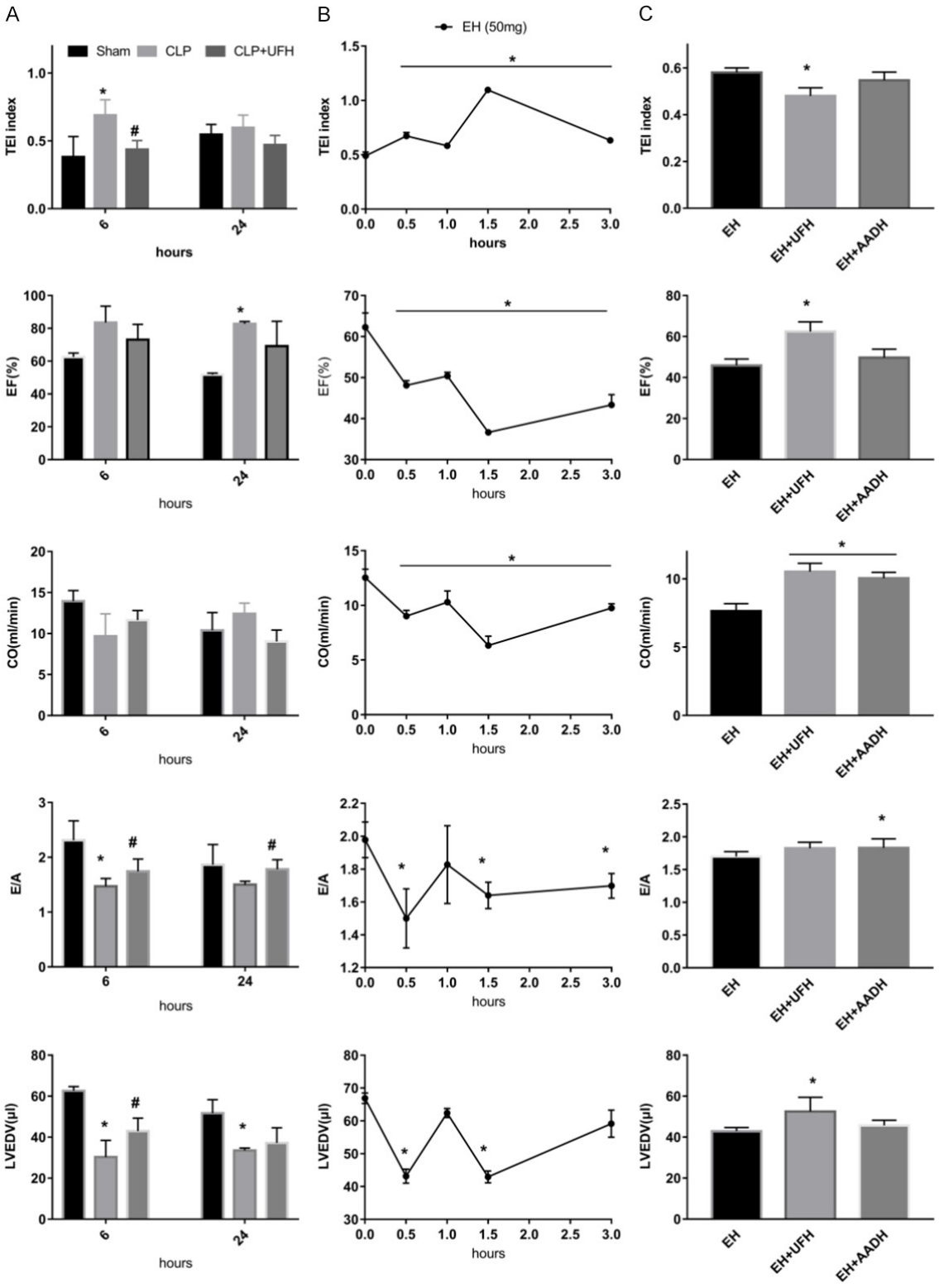


**Figure 2.** Echocardiography parameters in mice. Effects of sepsis on left ventricular function in mice at 6 h and 24 h after CLP and the protective effect of UFH (A, left panel). Mice were treated with UFH (3 mg/kg) by intraperitoneal injection at 4 h and 16 h after CLP to examine the potential protective effects (A). Effects of EH on left ventricular function in mice at designated time points (B). Beneficial role of histone neutralizing reagents (C). Both UFH and AADH (3 mg/kg) were injected intraperitoneally at 30 min before EH. EH, extracellular histones; EF, ejection fraction;

CO, cardiac output; LVEDV, left ventricular end diastolic volume; UFH, unfractionated heparin; AADH, antithrombin affinity-depleted heparin. Data are expressed as the mean ± SD (n=3 mice per group), *P<0.05 vs. sham (A, left panel), or respective control group (B, middle panel; C, right panel); #P<0.05 vs. respective CLP group (A, left panel).

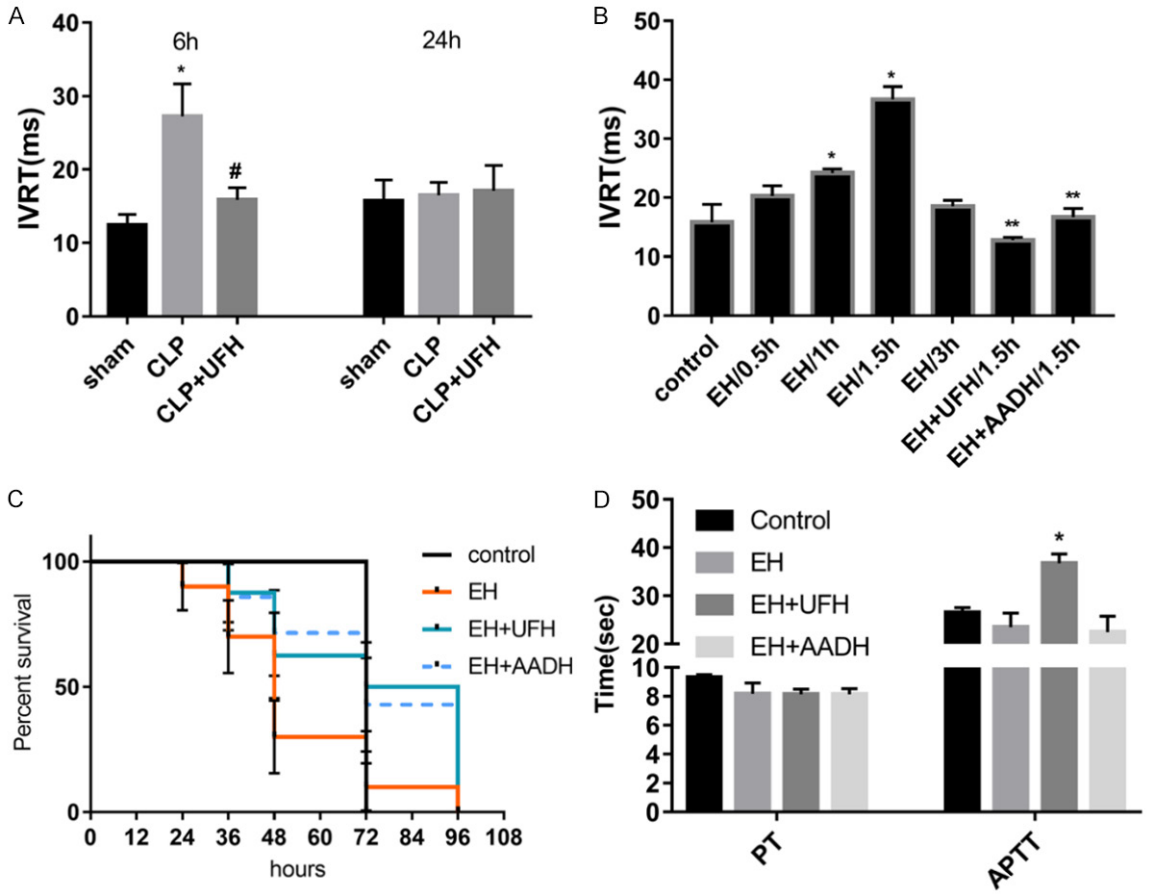


**Figure 3.** Effect of histone neutralizing agents on myocardial dysfunction and improved survival rate in CLP- or EH-treated mice. Alteration of IVRT in CLP (A) or EH-treated (B) mice at multiple time points. (C) There were 10 independent mice in each group. Both UFH and AADH (3 mg/kg, once every 12 h, 3 days in total) were administered 30 min before intraperitoneal injection of EH (50 mg/kg). (D) To confirm the non-anticoagulant effects of AADH, plasma was obtained 1.5 h after intraperitoneal histone (50 mg/kg) injection. Values are presented as the mean ± SD (n=3 in each group). *P<0.05 vs. control or sham group; #P<0.05 vs. CLP group; **P<0.05 vs. EH/1.5 h group. EH, extracellular histones; IVRT, isovolumic relaxation time; CLP, cecal ligation and puncture; UFH, unfractionated heparin; AADH, antithrombin affinity-depleted heparin; PT, prothrombin time; APTT, activated partial thromboplastin time.

coagulant activity was almost depleted (**Figure 3D**).

*Circulating histones were correlated with LVDD and apoptosis in CLP mice*

In order to investigate the association between circulating histones and apoptosis, we detected apoptotic factor levels in CLP mice using ELISA, qRT-PCR and western blot. Serum Bax levels were elevated significantly (P=0.018), whereas Bcl-2 did not decrease significantly after 6 h of CLP compared to the sham group (**Figure 4A-C**). There were significant correlations between circulating Bax and histone H4 ($r_s$=0.516, P=0.041), cTnT ($r_s$=0.497, P=0.005), and IVRT ($r_s$=0.414, P=0.023) at 6 h after CLP. However, there was no significant difference in caspase-3 levels among the three groups (**Figure 4A**). Compared to the sham group, the mRNA and protein levels of caspase-3 and Bax increased significantly, whereas Bcl-2 decreased significantly at 6 h after CLP (all P<0.05) (**Figure 4D**, **4E**). However, these harm-

**Table 1.** Echocardiography data of various changes in CLP mice

| | 6 hours | | | 24 hours | | |
|---|---|---|---|---|---|---|
| | sham | CLP | CLP + UFH | sham | CLP | CLP + UFH |
| HR, beats/min | 368±24 | 384±5 | 375±35 | 396±23 | 388±59 | 392±32 |
| Wall measurements | | | | | | |
| IVS-diastole, mm | 0.69±0.12 | 1.02±0.18* | 0.93±0.14 | 0.73±0.17 | 0.74±0.07 | 0.93±0.22 |
| IVS-systole, mm | 1.12±0.06 | 2.03±0.88* | 1.44±0.18 | 1.05±0.27 | 1.33±0.20 | 1.41±0.25 |
| LVPW-diastole, mm | 0.73±0.12 | 0.85±0.12* | 0.66±0.09 | 0.83±0.12 | 0.77±0.17 | 0.93±0.14 |
| LVPW-systole, mm | 1.05±0.15 | 1.34±0.21* | 1.00±0.26# | 1.17±0.24 | 1.28±0.22 | 1.26±0.23 |
| LVID-diastole, mm | 3.57±0.20 | 2.93±0.45* | 3.27±0.15 | 3.57±0.13 | 3.12±0.35 | 2.84±0.34 |
| LVID-systole, mm | 2.26±0.10 | 1.53±0.42* | 1.95±0.28 | 2.72±0.39 | 1.54±0.15 | 1.62±0.56 |
| Cardiac function | | | | | | |
| EF, % | 62.57±3.47 | 83.53±9.99 | 73.14±9.36 | 52.19±0.83 | 82.73±6.03* | 70.28±15.09 |
| FS, % | 31.05±5.66 | 52.60±12.22 | 46.60±9.02 | 35.53±12.39 | 50.16±2.26 | 41.82±13.79 |
| LVEDV, μl | 62.51±2.87 | 30.30±8.16* | 42.96±6.35# | 51.62±9.26 | 33.44±1.77 | 35.36±7.43 |
| LVESV, μl | 24.66±5.41 | 5.06±3.95 | 11.94±5.36 | 25.85±3.12 | 5.72±0.16 | 12.19±7.81 |
| CO, ml/min | 13.96±1,85 | 9.68±2.73 | 11.64±1.16 | 10.26±3.03 | 12.40±1.82 | 8.46±1.41 |
| SV, μl | 37.86±2.55 | 25.24±7.37 | 31.02±1.35 | 25.77±6.13 | 31.98±0.20 | 23.37±2.34 |
| Doppler imaging | | | | | | |
| IVRT, ms | 12.43±1.44 | 27.22±4.43* | 15.83±9.85# | 15.73±2.87 | 16.48±1.76 | 17.08±3.45 |
| IVCT, ms | 9.48±3.98 | 7.04±2.00 | 10.83±2.08 | 13.69±2.58 | 8.47±3.99 | 10.60±1.69 |
| ET, ms | 53.21±3.31 | 54.11±2.72 | 62.25±4.63 | 54.19±2.16 | 41.39±8.09 | 56.31±6.94 |
| Tei index | 0.38±0.15 | 0.69±0.11* | 0.43±0.07# | 0.55±0.08 | 0.60±0.09 | 0.47±0.09 |
| E/A ratio | 2.31±0.35 | 1.47±0.14* | 1.59±0.23# | 1.86±0.37 | 1.50±0.03 | 1.64±0.22 |

Data presented as mean ± SE, n=4-6, *P<0.05 vs. corresponding sham, #P<0.05 vs. corresponding CLP. HR: heart rate; IVS: interventricular septum; LVPW: left ventricular posterior wall; LVID: left ventricular interior diameter; EF: ejection fraction; FS: fraction shortening; LVEDV: left ventricular end diastolic volume; LVESV: left ventricular end systolic volume; CO: cardiac output; SV: stroke volume; IVRT: isovolumic relaxation time; IVCT: Isovolumic contraction time; ET: ejection time; CLP: cecal ligation and perforation.

ful effects were dramatically attenuated by UFH (**Figure 4A-E**).

*EH induced cardiomyocyte injury via different mechanisms*

*EH and cardiomyocyte apoptosis:* EH induced cardiomyocyte apoptosis in a concentration- and time-dependent manner (**Figure 5**). The incubation of cardiomyocytes with EH at 10 or 50 μg/mL showed no significant increase in cell apoptosis compared to the control group. However, 100 μg/mL of EH triggered a significant increase in apoptotic cells after 6 h of EH stimulation (**Figure 5A** and **5B**). As shown in **Figure 5C** and **5D**, cardiomyocyte apoptosis significantly increased at 0.5 h, peaked at 4 h, and lasted for 24 h.

The mRNA and protein levels of apoptotic factors in cardiomyocytes of different groups were then detected. The mRNA level of Bax, and the protein levels of cleaved caspase-3 and Bax were significantly increased at 6 h after EH stimulation and were decreased significantly after UFH treatment (P<0.05). However, there was no significant decrease in Bcl-2 mRNA level at 6 h after EH stimulation (**Figure 5E-I**).

Bax, cTnT, and TNFα levels in the cardiomyocyte supernatant were parallelly and concomitantly elevated 6 h after EH stimulation (P<0.05), which were partially reversed by UFH (**Figure 6A**, **6D**, and **6F**). There was a significant correlation between Bax and cTnT ($r_s$=0.804, P=0.002) or TNFα ($r_s$=0.604, P=0.038).

*LPS induced cardiomyocyte apoptosis depending on the presence of EH:* LPS is a bacterial wall endotoxin that can induce numerous pathophysiological conditions [13, 34]. We hypothesized that LPS induces cardiotoxicity via apoptosis. Cardiomyocytes were exposed to various concentrations of LPS (0.5-10 μg/mL)

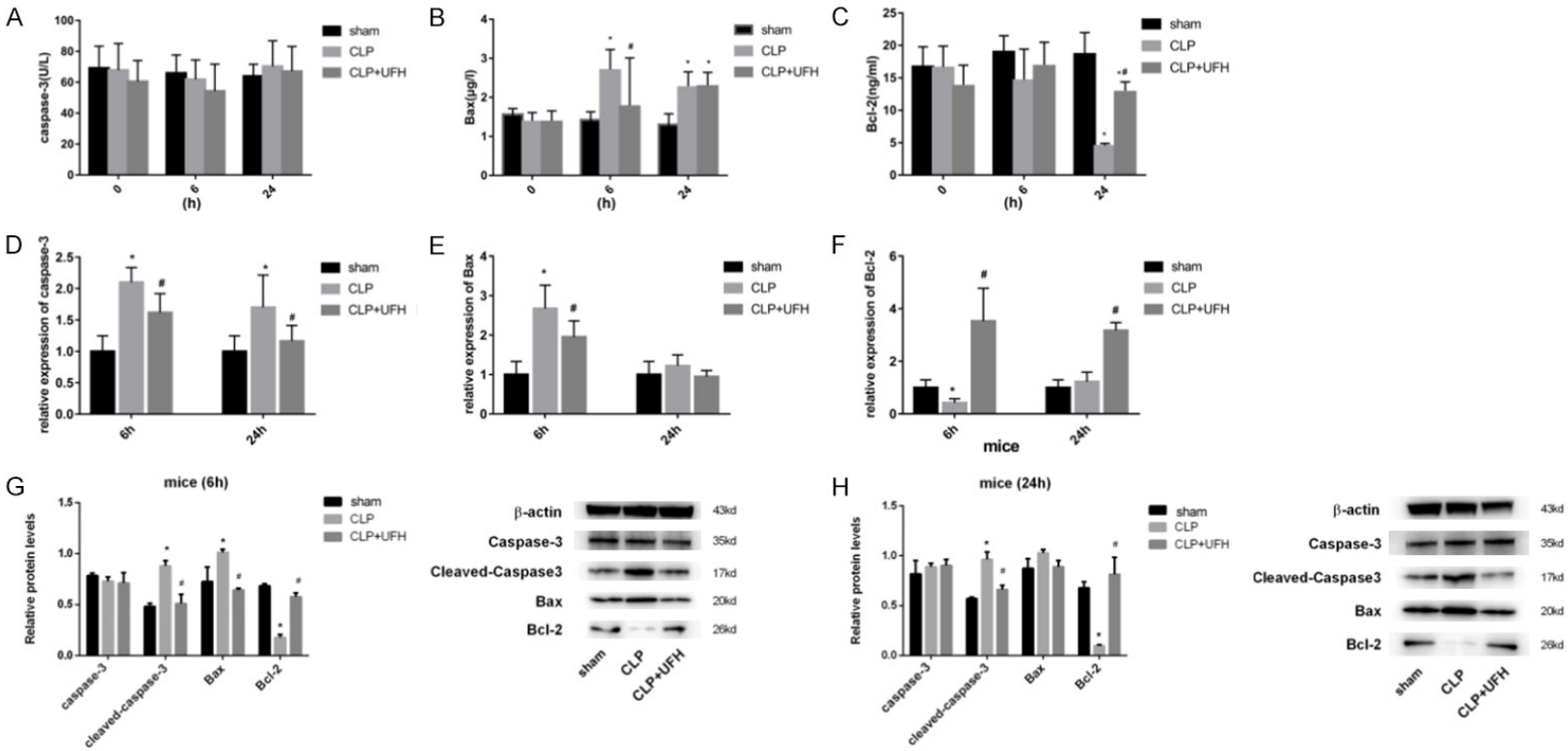


**Figure 4.** Relative mRNA and protein expression of caspase-3, Bax, and Bcl-2 in vivo or in vitro. Circulating levels of caspase-3 (A), Bax (B) and Bcl-2 (C) in the sham, CLP, and CLP + UFH groups at 6 h or 24 h after CLP detected by ELISA. (D-F) Relative mRNA expression of caspase-3, Bax and Bcl-2 in the left ventricle tissue of CLP mice at 6 h and 24 h detected by qRT-PCR. (G) Western blots and quantitative data of caspase-3, cleaved caspase-3, Bax, and Bcl-2 in left ventricle tissue from sham, CLP and CLP + UFH groups. (H) Western blots and quantitative data of caspase-3, cleaved caspase-3, Bax, and Bcl-2 in left ventricle tissue from sham, CLP and CLP + UFH groups at 24 h after CLP. Values are presented as the mean ± SD (n=3-9). GAPDH was used as an endogenous control of qRT-PCR. β-actin was regarded as an endogenous control of western blot. *P<0.05 vs. sham group at the same time; #P<0.05 vs. CLP group at the same time. UFH, unfractionated heparin; CLP, cecal ligation and puncture. UFH (3 mg/kg) was intraperitoneally injected at 4 h and 16 h after CLP.

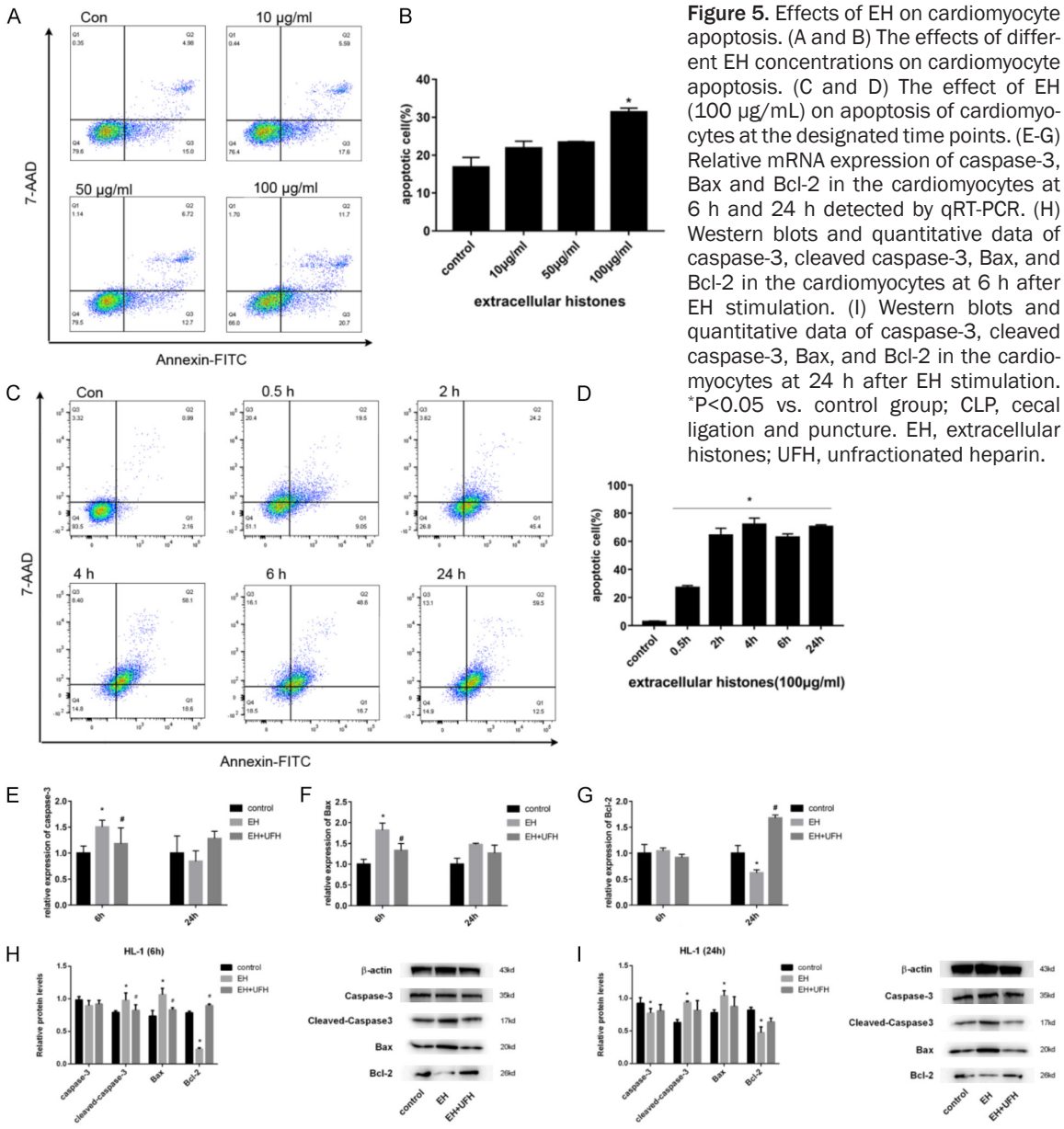


**Figure 5.** Effects of EH on cardiomyocyte apoptosis. (A and B) The effects of different EH concentrations on cardiomyocyte apoptosis. (C and D) The effect of EH (100 μg/mL) on apoptosis of cardiomyocytes at the designated time points. (E-G) Relative mRNA expression of caspase-3, Bax and Bcl-2 in the cardiomyocytes at 6 h and 24 h detected by qRT-PCR. (H) Western blots and quantitative data of caspase-3, cleaved caspase-3, Bax, and Bcl-2 in the cardiomyocytes at 6 h after EH stimulation. (I) Western blots and quantitative data of caspase-3, cleaved caspase-3, Bax, and Bcl-2 in the cardiomyocytes at 24 h after EH stimulation. *P<0.05 vs. control group; CLP, cecal ligation and puncture. EH, extracellular histones; UFH, unfractionated heparin.

and no significant cardiomyocyte apoptosis was observed (data not shown). However, when LPS (even at a concentration of 1 μg/mL) was co-incubated with EH, the apoptotic rate of cardiomyocytes was significantly increased compared to that in the EH-incubated group (P< 0.001). Therefore, LPS may synergize with EH to further increase the apoptosis of cardiomyocytes. This process was partially reversed by UFH (**Figure 7**).

*EH increased reactive oxygen species (ROS) in cardiomyocytes:* Total ROS levels were measured to assess the effects of EH on ROS production in cardiomyocytes. The results showed that ROS levels were elevated in cardiomyocytes in a time-dependent manner, which was initiated at 0.5 h after EH stimulation, and peaked at 2-4 h compared to the control group (P=0.021). UFH reduced the extent of ROS elevation (**Figure 8**). Therefore, EH might lead to cardiomyocyte apoptosis by increasing ROS levels.

## Discussion

The present study revealed that EH resulted in LVDD in sepsis, which might be associated with EH-induced apoptosis. Further experiments found that this apoptosis could be related to

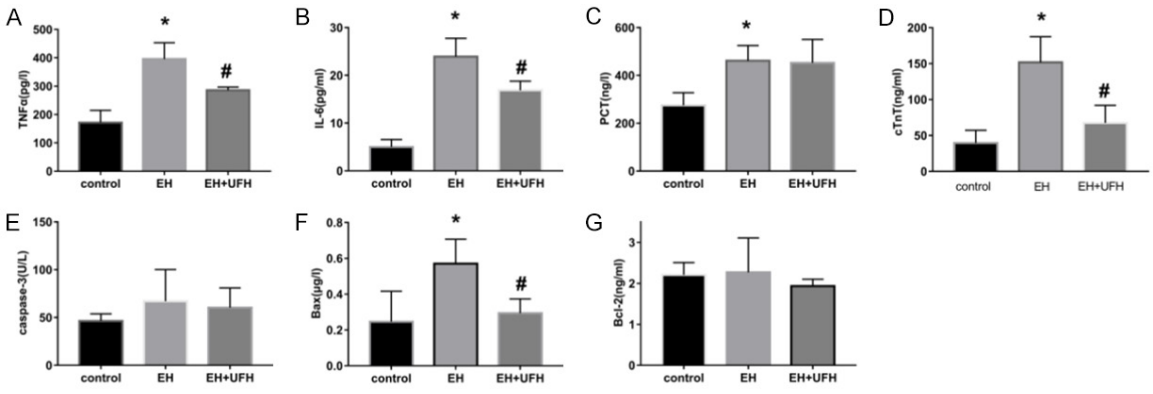


**Figure 6.** Effects of EH on related protein in the supernatant of cardiomyocytes. Effects of EH on TNFα, IL-6, procalcitonin (PCT), LPS, apoptotic proteins (caspase-3, Bax, and Bcl-2), and cTnT levels in the supernatant of cardiomyocytes. Values are presented as the mean ± SD (n=3-6). EH, extracellular histones; UFH, unfractionated heparin. *P<0.05 vs. control group; #P<0.05 vs. EH group.

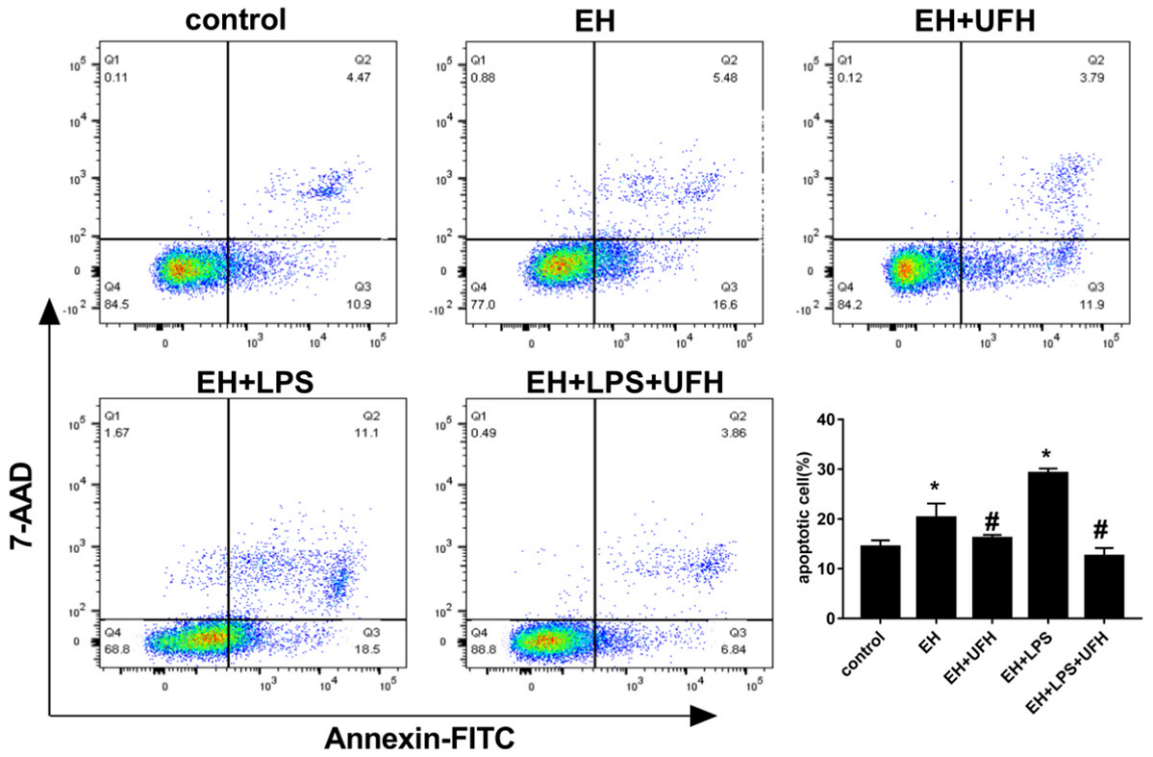


**Figure 7.** Effects of EH on the apoptotic rate in cardiomyocytes. To further demonstrate the effects of EH on apoptosis in cardiomyocytes, we first pre-incubated cardiomyocytes with UFH (200 μg/mL) for half an hour in the UFH group, followed by EH (100 μg/mL) or EH + LPS (1 μg/mL) stimulation. UFH can protect cardiomyocytes against apoptosis induced by EH in the presence or absence of LPS. Values are presented as the mean ± SD (n=3-5). EH, extracellular histones; UFH, unfractionated heparin; LPS, lipopolysaccharides *P<0.05 vs. control group, #P<0.05 vs. designated EH or EH + LPS group.

the early direct damage to the myocardial cell membrane or the early increase in TNFα and Bax expression. UFH, one of the neutralizing reagents of EH, could improve SMI *in vivo* and *in vitro*.

*EH induced LVDD in mice with sepsis*

In patients with sepsis, the incidence of LVDD is higher than that of systolic dysfunction, and the incidence of LVDD in patients with sepsis

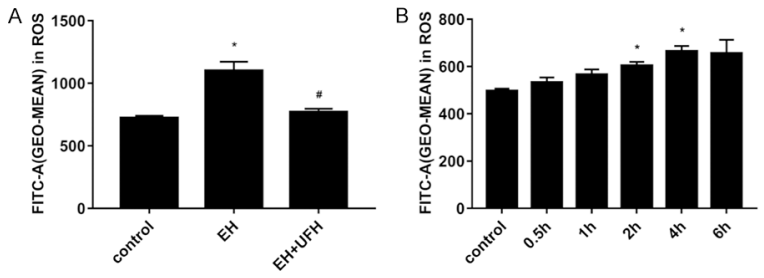


**Figure 8.** Effects of EH on ROS in cardiomyocytes. (A) Effects of EH on ROS in cardiomyocytes 4 h after EH stimulation. (B) Effect of EH on ROS in cardiomyocytes at multiple time points. Values are presented as the mean ± SD (n=3-6 in each group). EH, extracellular histones; UFH, unfractionated heparin; ROS: Reactive oxygen species. *P<0.05 vs. control group; #P<0.05 vs. EH group.

has been seriously underestimated in recent years [7, 10, 35, 36]. Echocardiography, which can reveal early alteration of SMI, has become the gold standard for SMI diagnosis [4, 5, 37]. E/A ratio, IVRT, and LVEDV are commonly used indicators for assessing LVDD [36, 38].

Patients who died of septic shock had significantly lower LVEDV than those who recovered, indicating that LVEDV is a prognostic factor in patients with sepsis [39]. Fattahi et al. [20, 37] showed that CLP mice presented a decrease in LVEDV over 24 h. Our results also demonstrated that LVEDV significantly decreased in CLP mice after 6 h or in EH-treated mice after 1.5 h compared to the sham or control groups. It may be related to vasodilation, decreased blood return to the heart, or pulmonary vascular obstruction caused by EH [8, 25, 39]. EH (≥60 mg/kg) can induce pulmonary vascular obstruction by increasing neutrophil congestion, NETosis, and thrombosis [8]. Nakahara et al. [25] indicated that recombinant thrombomodulin rescued mice with sepsis from lethal thromboembolism by suppressing histone-induced injury. IVRT, a preload-independent variable, has also been used to reflect LVDD, which is prolonged in patients with sepsis and mice [9, 20, 34, 37, 40]. In the present study, IVRT was increased 6 h after CLP or 1.5 h after EH administration. Moreover, there were significant correlations between circulating histones and cTnT, E/A ratio, and IVRT in CLP mice. Therefore, EH is involved in LVDD during sepsis.

Circulating histones and Bax protein levels were elevated in parallel and concomitantly at 6 h after CLP, with the elevations partially reversed by UFH in our experiments. Further study showed that there was a correlation between circulating histones and Bax in CLP mice, which might indicate that EH induced apoptosis by increasing Bax protein levels, resulting in LVDD in mice with sepsis.

*EH directly induced cardiomyocyte apoptosis at the early stage*

Myofilament properties play a central role in the control of cardiac relaxation. Cardiomyocyte apoptosis induces the cleavage of cardiac myofilament components, causing diastolic dysfunction [11, 17]. In our results, cardiomyocytes presented a significant apoptosis 0.5 h after EH stimulation, with a peak value at 4 h. Alhamdi et al. [18] found that EH was directly concentrated on the plasma membrane 10 min after administration, and entered cardiomyocytes 30 min later, indicating that the integrity of the cardiomyocyte membrane was destroyed. Farrahi et al. [20] showed that rat cardiomyocytes exposed to EH had bleb formation on the surfaces of cardiomyocytes, suggesting that EH may perturb the cardiomyocyte membrane. EH acts before any inflammatory mediators are triggered [26, 41]. Moreover, EH can elevate cytosolic calcium, reduce agonist responses in platelets, and decrease the viability of murine tubular epithelial cells or renal endothelial cells [23, 42]. Furthermore, Nakahara et al. [25] indicated that EH led to right-sided heart failure within 30 min, which may be related to early death.

Myocardial edema caused by inflammation-induced vascular leakage may also affect cardiac compliance in patients with sepsis [43, 44]. However, our results suggested that the left ventricular posterior wall diastolic thickness was significantly increased after 6 h of CLP, whereas there was no significant difference after 1.5 h of EH administration (data not shown) comparesd to the control group. Therefore, EH directly stimulated cardiomyocytes, leading to apoptosis rather than via indirect stimulation through inflammatory mediators at the early stage.

*EH induced cardiomyocyte apoptosis via Bax-TNFα pathway at the early stage*

Our results demonstrated that inflammatory mediators, such as IL-6 and TNFα, were elevated at 6 h after EH stimulation in the supernatant of cardiomyocytes. In addition, TNFα and Bax levels were parallelly and concomitantly elevated in both CLP mice and EH-treated cardiomyocytes. In particular, these elevations were partially reversed by the UFH. Wang et al. [45] reported that TNFα was positively correlated with Bax at both the mRNA and protein levels in burned rats. Our results are consistent with those reported above.

TNFα is present in the circulation, which can be locally produced by cardiomyocytes and released 2 h after LPS or CLP induction [12, 21, 37, 46]. As an important inflammatory mediator, it is involved in the development of SMI [12, 15, 34]. A recent study reported that stromal cell-derived factor-1 induced TNF-mediated apoptosis in cardiac myocytes 24 h after stimulation; however, apoptosis significantly decreased when TNFα expression was neutralized [15]. TNFα can reduce the calcium concentration in the sarcoplasmic reticulum of myocardial cells during systole and decrease the peak value of L-form calcium, resulting in myocardial dysfunction [47]. Furthermore, TNF-α and Bax were concomitantly elevated in LPS-induced H9C2 cells 24 h after LPS stimulation, whereas growth arrest-specific gene 6 attenuated TNFα and Bax expression [13]. Zhang et al. [48] found that TNFα induced apoptosis via the JNK/Bax-dependent pathway in differentiated PC12 cells. Taken together, these results suggest that EH may upregulate Bax protein expression via TNFα to increase cardiomyocyte apoptosis, resulting in cardiac injury at an early stage *in vivo* and *in vitro*. The potential mechanisms of EH-induced LVDD in sepsis are shown in Figure S3.

*Limitations*

There were some limitations in our study. Histone, cTnT, and apoptotic protein levels in EH-treated mice, and the correlation analysis between these parameters and LV diastolic function, were not detected. Additionally, we selected E/A, LVEDV, and IVRT to assess LV diastolic function rather than E/e', which is a better predictor of hospital mortality [7, 10]. Furthermore, there was an interaction between ventricle and atrium function. The alterations in the right ventricle or left atrium were not analyzed.

## Conclusion

In conclusion, limited data in our experiments revealed that EH is associated with LVDD in sepsis, which may be associated with EH-induced apoptosis. Apoptosis may be related to direct damage to the cardiomyocyte membrane or increased expression of TNFα and Bax. Our research provides a new theoretical basis for the pathogenesis of SMI.

## Acknowledgements

We thank Professor Shuzhang Cui, Yanfen Chai and Songtao Shou of Department of Emergency in Tianjin Medical University General Hospital for revising the manuscript. This study was supported by grants from the National Natural Science Foundation of China (No. 81871593, 81700304, and 81900314), Peking Union Medical Foundation-Ruiyi Emergency Medical Research Fund (No. R2018006), Tianjin Binhai New Area Health Commission Science and Technology Project (No. 2018BWKZ008), The Scientific Research Fund Project of Key Laboratory of Second Hospital of Tianjin Medical University (No. 2019ZDSYS11) and PhD Research Foundation of Affiliated Hospital of Jining Medical University (No.: 2021-BS-005). The funders had no role in study design, data collection, data analysis, data interpretation, or writing of the manuscript.

## Disclosure of conflict of interest

None.

## Abbreviations

AADH, Antithrombin affinity-depleted heparin; APTT, Activated partial thromboplastin time; CLP, Cecal ligation and perforation; CO, Cardiac output; cTnT, Cardiac troponin T; EF, Ejection fraction; EH, Extracellular histones; ELISA, Enzyme-linked immunosorbent assay; GAPDH, Glyceraldehyde 3-phosphate dehydrogenase; IL-6, Interleukin-6; IP, Intraperitoneal; IVRT, Isovolumic relaxation time; LPS, Lipopolysaccharide; LVDD, Left ventricular diastolic dysfunction; LVEDV, Left ventricular end diastolic volume; PCT, Procalcitonin; PT, Prothrombin

time; ROS, Reactive oxygen species; SDF-1, Stromal cell-derived factor-1; SMI, Septic myocardial injury; TBST, Tris-buffered saline with Tween; TLR, Toll-like receptor; TNFα, Tumor necrosis factor α; UFH, Unfractionated heparin.

**Address correspondence to:** Guangping Li and Xue Liang, Department of Cardiology, Tianjin Key Laboratory of Ionic-Molecular Function of Cardiovascular Disease, Tianjin Institute of Cardiology, The Second Hospital of Tianjin Medical University, No 23, Pingjiang Road, Hexi District, Tianjin 300211, People's Republic of China. Tel: +86-022-88328700; Fax: +86-022-28261158; E-mail: tic_tjcardiol@126.com (GPL); liangxue19841219@126.com (XL)

## References

[1] Singer M, Deutschman CS, Seymour CW, Shankar-Hari M, Annane D, Bauer M, Bellomo R, Bernard GR, Chiche JD, Coopersmith CM, Hotchkiss RS, Levy MM, Marshall JC, Martin GS, Opal SM, Rubenfeld GD, van der Poll T, Vincent JL and Angus DC. The Third International Consensus definitions for sepsis and septic shock (Sepsis-3). JAMA 2016; 315: 801-810.

[2] Kakihana Y, Ito T, Nakahara M, Yamaguchi K and Yasuda T. Sepsis-induced myocardial dysfunction: pathophysiology and management. J Intensive Care 2016; 4: 22.

[3] Ming S, Li M, Wu M, Zhang J, Zhong H, Chen J, Huang Y, Bai J, Huang L, Chen J, Lin Q, Liu J, Tao J, He D and Huang X. Immunoglobulin-like transcript 5 inhibits macrophage-mediated bacterial killing and antigen presentation during sepsis. J Infect Dis 2019; 220: 1688-1699.

[4] Kim JS, Kim M, Kim YJ, Ryoo SM, Sohn CH, Ahn S and Kim WY. Troponin testing for assessing sepsis-induced myocardial dysfunction in patients with septic shock. J Clin Med 2019; 8: 239.

[5] Fattahi F and Ward PA. Complement and sepsis-induced heart dysfunction. Mol Immunol 2017; 84: 57-64.

[6] Pischke SE, Hestenes S, Johansen HT, Fure H, Bugge JF, Espinoza A, Skulstad H, Edvardsen T, Fosse E, Mollnes TE, Halvorsen PS and Nielsen EW. Sepsis causes right ventricular myocardial inflammation independent of pulmonary hypertension in a porcine sepsis model. PLoS One 2019; 14: e0218624.

[7] Lanspa MJ, Olsen TD, Wilson EL, Leguyader ML, Hirshberg EL, Anderson JL, Brown SM and Grissom CK. A simplified definition of diastolic function in sepsis, compared against standard definitions. J Intensive Care 2019; 7: 14.

[8] Alhamdi Y, Zi M, Abrams ST, Liu T, Su D, Welters I, Dutt T, Cartwright EJ, Wang G and Toh CH. Circulating histone concentrations differentially affect the predominance of left or right ventricular dysfunction in critical illness. Crit Care Med 2016; 44: e278-288.

[9] Landesberg G, Gilon D, Meroz Y, Georgieva M, Levin PD, Goodman S, Avidan A, Beeri R, Weissman C, Jaffe AS and Sprung CL. Diastolic dysfunction and mortality in severe sepsis and septic shock. Eur Heart J 2012; 33: 895-903.

[10] Rolando G, Espinoza ED, Avid E, Welsh S, Pozo JD, Vazquez AR, Arzani Y, Masevicius FD and Dubin A. Prognostic value of ventricular diastolic dysfunction in patients with severe sepsis and septic shock. Rev Bras Ter Intensiva 2015; 27: 333-339.

[11] Lancel S, Joulin O, Favory R, Goossens JF, Kluza J, Chopin C, Formstecher P, Marchetti P and Neviere R. Ventricular myocyte caspases are directly responsible for endotoxin-induced cardiac dysfunction. Circulation 2005; 111: 2596-2604.

[12] Zhong J, Tan Y, Lu J, Liu J, Xiao X, Zhu P, Chen S, Zheng S, Chen Y, Hu Y and Guo Z. Therapeutic contribution of melatonin to the treatment of septic cardiomyopathy: a novel mechanism linking Ripk3-modified mitochondrial performance and endoplasmic reticulum function. Redox Biol 2019; 26: 101287.

[13] Li M, Ye J, Zhao GJ, Hong GL, Hu XY, Cao KQ, Wu Y and Lu ZQ. Gas6 attenuates lipopolysaccharide-induced TNF-α expression and apoptosis in H9C2 cells through NF-κB and MAPK inhibition via the Axl_PI3K_Akt pathway. Int J Mol Med 2019; 44: 982-994.

[14] Zhang X, Zhang X, Xiong Y, Xu C, Liu X, Lin J, Mu G, Xu S and Liu W. Sarcolemmal ATP-sensitive potassium channel protects cardiac myocytes against lipopolysaccharide-induced apoptosis. Int J Mol Med 2016; 38: 758-766.

[15] Jarrah AA, Schwarskopf M, Wang ER, LaRocca T, Dhume A, Zhang S, Hadri L, Hajjar RJ, Schecter AD and Tarzami ST. SDF-1 induces TNF-mediated apoptosis in cardiac myocytes. Apoptosis 2018; 23: 79-91.

[16] Xu X, Liu Q, He S, Zhao J, Wang N, Han X and Guo Y. Qiang-xin 1 formula prevents sepsis-induced apoptosis in murine cardiomyocytes by suppressing endoplasmic reticulum- and mitochondria-associated pathways. Front Pharmacol 2018; 9: 818.

[17] Periasamy M and Janssen PM. Molecular basis of diastolic dysfunction. Heart Fail Clin 2008; 4: 13-21.

[18] Alhamdi Y, Abrams ST, Cheng Z, Jing S, Su D, Liu Z, Lane S, Welters I, Wang G and Toh CH. Circulating histones are major mediators of cardiac injury in patients with sepsis. Crit Care Med 2015; 43: 2094-2103.

[19] Kalbitz M, Grailer JJ, Fattahi F, Jajou L, Herron TJ, Campbell KF, Zetoune FS, Bosmann M, Sarma JV, Huber-Lang M, Gebhard F, Loaiza R, Valdivia HH, Jalife J, Russell MW and Ward PA. Role of extracellular histones in the cardiomyopathy of sepsis. FASEB J 2015; 29: 2185-2193.

[20] Fattahi F, Russell MW, Malan EA, Parlett M, Abe E, Zetoune FS and Ward PA. Harmful roles of TLR3 and TLR9 in cardiac dysfunction developing during polymicrobial sepsis. Biomed Res Int 2018; 2018: 4302726.

[21] Fattahi F, Frydrych LM, Bian G, Kalbitz M, Herron TJ, Malan EA, Delano MJ and Ward PA. Role of complement C5a and histones in septic cardiomyopathy. Mol Immunol 2018; 102: 32-41.

[22] Liu Z, Yue S, Chen X, Kubin T and Braun T. Regulation of cardiomyocyte polyploidy and multinucleation by CyclinG1. Circ Res 2010; 106: 1498-1506.

[23] Vulliamy P, Gillespie S, Armstrong PC, Allan HE, Warner TD and Brohi K. Histone H4 induces platelet ballooning and microparticle release during trauma hemorrhage. Proc Natl Acad Sci U S A 2019; 116: 17444-17449.

[24] Paues Goranson S, Thalin C, Lundstrom A, Hallstrom L, Lasselin J, Wallen H, Soop A and Mobarrez F. Circulating H3Cit is elevated in a human model of endotoxemia and can be detected bound to microvesicles. Sci Rep 2018; 8: 12641.

[25] Nakahara M, Ito T, Kawahara K, Yamamoto M, Nagasato T, Shrestha B, Yamada S, Miyauchi T, Higuchi K, Takenaka T, Yasuda T, Matsunaga A, Kakihana Y, Hashiguchi T, Kanmura Y and Maruyama I. Recombinant thrombomodulin protects mice against histone-induced lethal thromboembolism. PLoS One 2013; 8: e75961.

[26] Pan B, Alam HB, Chong W, Mobley J, Liu B, Deng Q, Liang Y, Wang Y, Chen E, Wang T, Tewari M and Li Y. CitH3: a reliable blood biomarker for diagnosis and treatment of endotoxic shock. Sci Rep 2017; 7: 8972.

[27] Wang L, Wang J, Guo F, Wang ZY and Song RW. Effects and clinical value of Xuebijing injection on plasma histone H4 in patients with sepsis. Tianjin Journal of Traditional Chinese Medicine 2019; 36: 5.

[28] Fattahi F, Grailer JJ, Jajou L, Zetoune FS, Andjelkovic AV and Ward PA. Organ distribution of histones after intravenous infusion of FITC histones or after sepsis. Immunol Res 2015; 61: 177-186.

[29] Vogel B, Shinagawa H, Hofmann U, Ertl G and Frantz S. Acute DNase1 treatment improves left ventricular remodeling after myocardial infarction by disruption of free chromatin. Basic Res Cardiol 2015; 110: 15.

[30] Toscano MG, Ganea D and Gamero AM. Cecal ligation puncture procedure. J Vis Exp 2011: 2860.

[31] Wang F, Zhang N, Li B, Liu L, Ding L, Wang Y, Zhu Y, Mo X and Cao Q. Heparin defends against the toxicity of circulating histones in sepsis. Front Biosci (Landmark Ed) 2015; 20: 1259-1270.

[32] Wildhagen KC, García de Frutos P, Reutelingsperger CP, Schrijver R, Aresté C, Ortega-Gómez A, Deckers NM, Hemker HC, Soehnlein O and Nicolaes GA. Nonanticoagulant heparin prevents histone-mediated cytotoxicity in vitro and improves survival in sepsis. Blood 2014; 123: 1098-1101.

[33] Wen Z, Lei Z, Yao L, Jiang P, Gu T, Ren F, Liu Y, Gou C, Li X and Wen T. Circulating histones are major mediators of systemic inflammation and cellular injury in patients with acute liver failure. Cell Death Dis 2016; 7: e2391.

[34] Samokhvalov V, Jamieson KL, Darwesh AM, Keshavarz-Bahaghighat H, Lee TYT, Edin M, Lih F, Zeldin DC and Seubert JM. Deficiency of soluble epoxide hydrolase protects cardiac function impaired by LPS-induced acute inflammation. Front Pharmacol 2018; 9: 1572.

[35] Beraud AS, Guillamet CV, Hammes JL, Meng L, Nicolls MR and Hsu JL. Efficacy of transthoracic echocardiography for diagnosing heart failure in septic shock. Am J Med Sci 2014; 347: 295-298.

[36] Moon YJ, Kim JW, Bang YS, Lim YS, Ki Y and Sang BH. Prediction of all-cause mortality after liver transplantation using left ventricular systolic and diastolic function assessment. PLoS One 2019; 14: e0209100.

[37] Hoffman M, Kyriazis ID, Lucchese AM, de Lucia C, Piedepalumbo M, Bauer M, Schulze PC, Bonios MJ, Koch WJ and Drosatos K. Myocardial strain and cardiac output are preferable measurements for cardiac dysfunction and can predict mortality in septic mice. J Am Heart Assoc 2019; 8: e012260.

[38] Rodriguez-Gonzalez M, Perez-Reviriego AA, Castellano-Martinez A, Lubian-Lopez S and Benavente-Fernandez I. Left ventricular dysfunction and plasmatic NT-proBNP are associated with adverse evolution in respiratory syncytial virus bronchiolitis. Diagnostics (Basel) 2019; 9: 85.

[39] Jardin F, Fourme T, Page B, Loubieres Y, Vieillard-Baron A, Beauchet A and Bourdarias JP. Persistent preload defect in severe sepsis despite fluid loading: a longitudinal echocardiographic study in patients with septic shock. Chest 1999; 116: 1354-1359.

[40] Fattahi F, Kalbitz M, Malan EA, Abe E, Jajou L, Huber-Lang MS, Bosmann M, Russell MW, Zetoune FS and Ward PA. Complement-induced activation of MAPKs and Akt during

sepsis: role in cardiac dysfunction. FASEB J 2017; 31: 4129-4139.
[41] Abrams ST, Zhang N, Manson J, Liu T, Dart C, Baluwa F, Wang SS, Brohi K, Kipar A, Yu W, Wang G and Toh CH. Circulating histones are mediators of trauma-associated lung injury. Am J Respir Crit Care Med 2013; 187: 160-169.
[42] Ekaney ML, Otto GP, Sossdorf M, Sponholz C, Boehringer M, Loesche W, Rittirsch D, Wilharm A, Kurzai O, Bauer M and Claus RA. Impact of plasma histones in human sepsis and their contribution to cellular injury and inflammation. Crit Care 2014; 18: 543.
[43] De Schryver N, Hoton D, Castanares-Zapatero D and Hantson P. Acute ventricular wall thickening: sepsis, thrombotic microangiopathy, or myocarditis? Case Rep Cardiol 2015; 2015: 275825.
[44] Chagnon F, Bentourkia M, Lecomte R, Lessard M and Lesur O. Endotoxin-induced heart dysfunction in rats: assessment of myocardial perfusion and permeability and the role of fluid resuscitation. Crit Care Med 2006; 34: 127-33.
[45] Wang Z, Fang J and Xiao J. Correlation of the expression of inflammatory factors with expression of apoptosis-related genes Bax and Bcl-2, in burned rats. Exp Ther Med 2019; 17: 1790-1796.
[46] Allam R, Scherbaum CR, Darisipudi MN, Mulay SR, Hagele H, Lichtnekert J, Hagemann JH, Rupanagudi KV, Ryu M, Schwarzenberger C, Hohenstein B, Hugo C, Uhl B, Reichel CA, Krombach F, Monestier M, Liapis H, Moreth K, Schaefer L and Anders HJ. Histones from dying renal cells aggravate kidney injury via TLR2 and TLR4. J Am Soc Nephrol 2012; 23: 1375-1388.
[47] Yang F, Zhao LN, Sun Y and Chen Z. Levosimendan as a new force in the treatment of sepsis-induced cardiomyopathy: mechanism and clinical application. J Int Med Res 2019; 47: 1817-1828.
[48] Zhang L, Xing D, Liu L, Gao X and Chen M. TNF-α induces apoptosis through JNK/Bax-dependent pathway in differentiated, but not Naïve PC12 cells. Cell Cycle 2007; 6: 1479-1486.

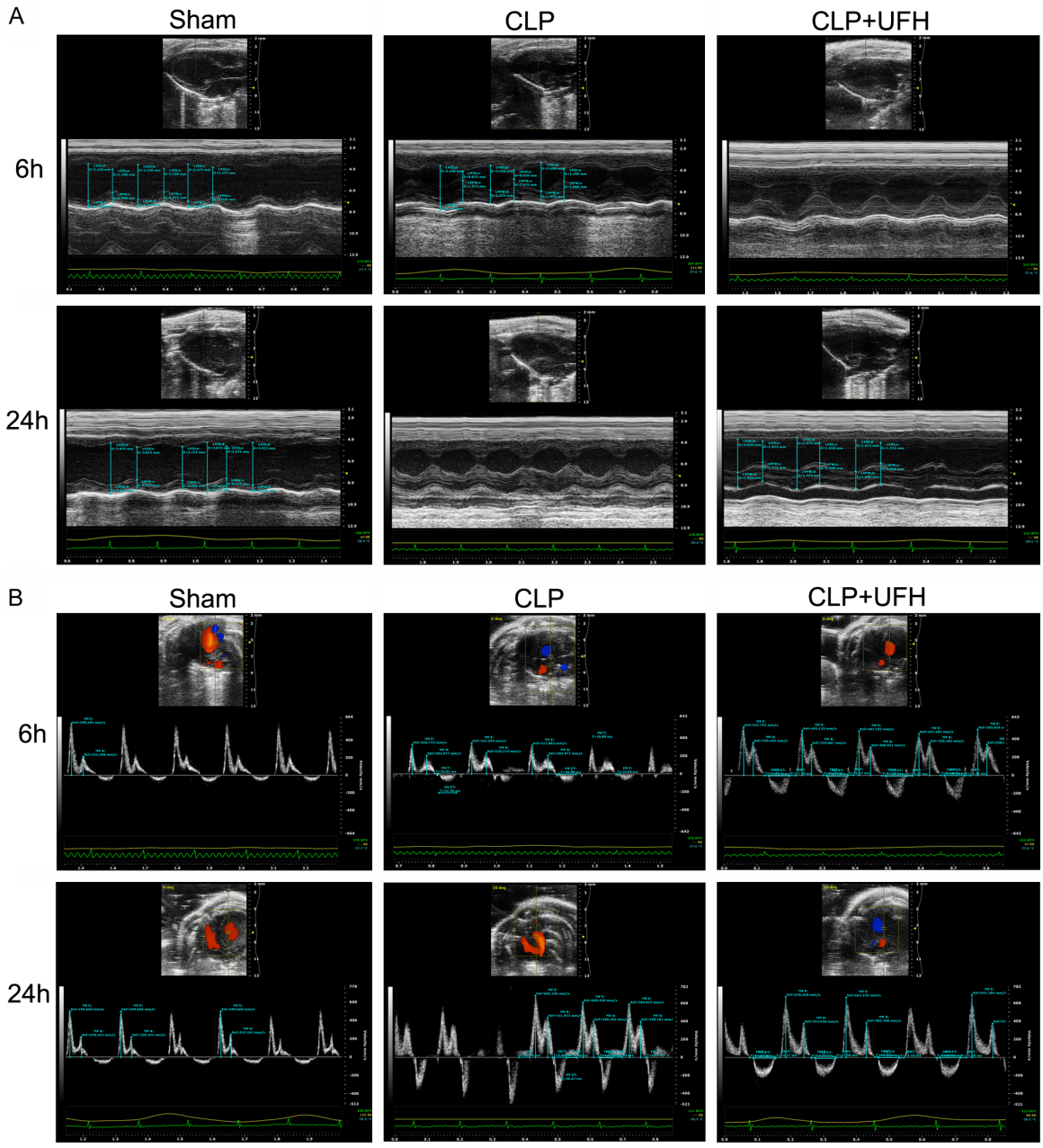


**Figure S1.** Echocardiography of mice in sham, CLP and CLP + UFH groups. (A) Echocardiography displays LVEDV and EF of mice in sham, CLP and CLP + UFH groups at 6 h and 24 h. (B) Echocardiography displays E/A ratio, Tei index and IVRT of mice in sham, CLP and CLP + UFH groups at 6 h and 24 h. CLP, cecal ligation and puncture; E/A ratio, the ratio between E-wave and A-wave; EF, ejection fraction; IVRT, isovolumic relaxation time; LVEDV, left ventricular end diastolic volume; UFH, unfractionated heparin.

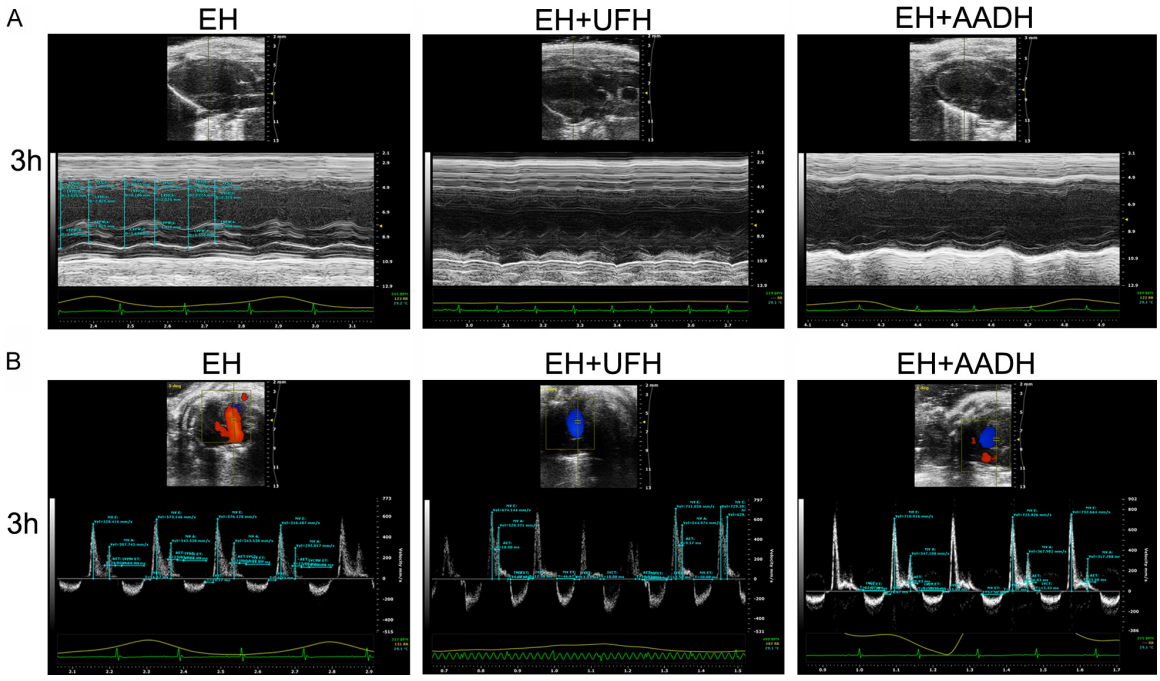


**Figure S2.** Echocardiography of mice in EH, EH + UFH and EH + AADH groups at 3 h. (A) Echocardiography displays LVEDV and EF of mice. (B) Echocardiography displays E/A ratio, Tei index and IVRT of mice. AADH, antithrombin affinity-depleted heparin; E/A ratio, the ratio between E-wave and A-wave; EF, ejection fraction; EH, extracellular histones; IVRT, isovolumic relaxation time; LVEDV, left ventricular end diastolic volume; UFH, unfractionated heparin.

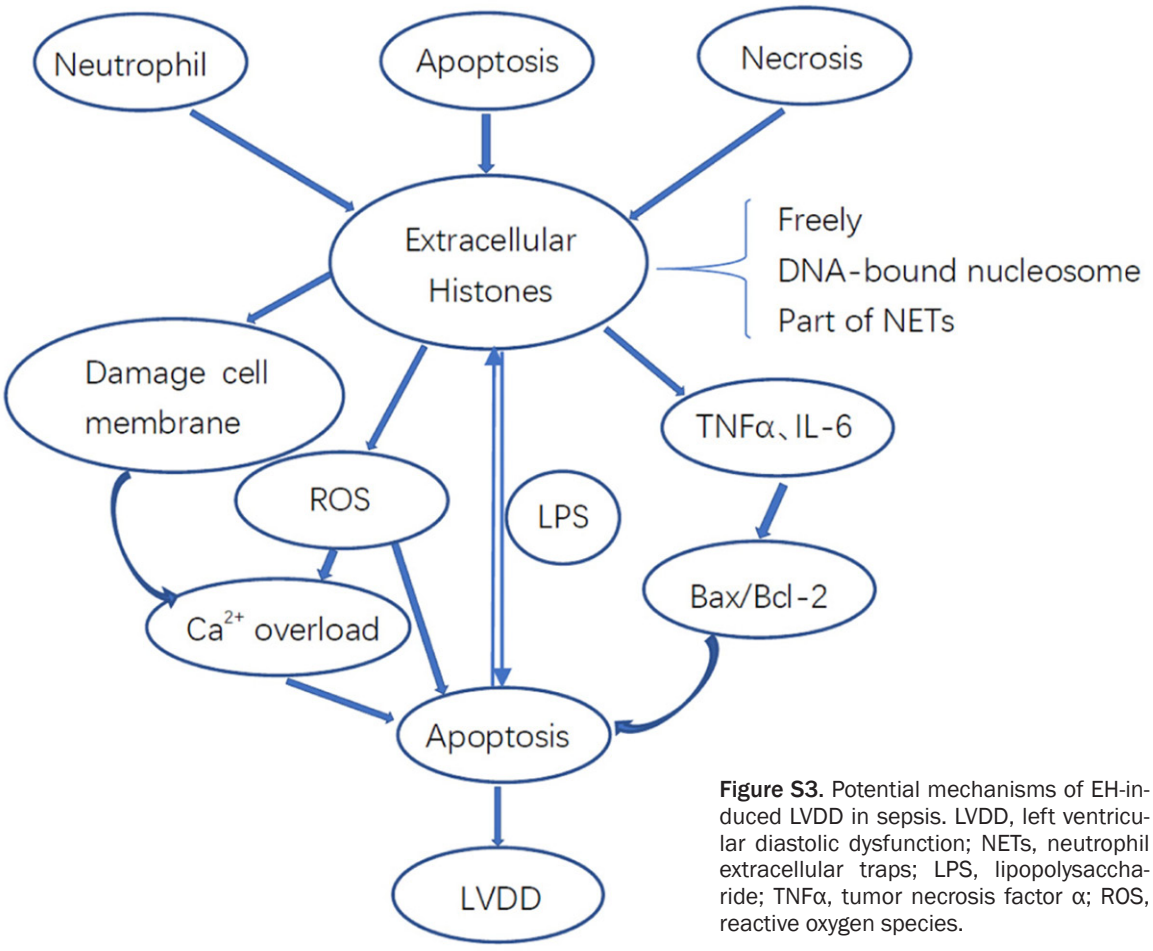


**Figure S3.** Potential mechanisms of EH-induced LVDD in sepsis. LVDD, left ventricular diastolic dysfunction; NETs, neutrophil extracellular traps; LPS, lipopolysaccharide; TNFα, tumor necrosis factor α; ROS, reactive oxygen species.